Robustness of High-Resolution Channel Parameter Estimators in the Presence of Dense Multipath Components

E. Tanghe, D. P. Gaillot, W. Joseph, M. Liénard, P. Degauque, and L. Martens

Abstract: The estimation accuracy of specular multipath components in radio channels that include dense multipath is investigated. Classical multipath estimation algorithms such as ESPRIT and SAGE do not include dense multipath in their signal model whereas recent ones, such as RiMAX, do. These estimation algorithms are applied to a-priori known synthetic channels which include both specular components (SCs) and dense multipath components (DMC). The estimation errors of the SCs are computed as a function of the DMC power to evaluate the estimator's robustness. The results of this work clearly indicate large estimation errors for the SC parameters when the estimator does not include DMC in its data model.

Introduction: The signal model of conventional high-resolution multipath estimation algorithms such as ESPRIT [1] and SAGE [2] presupposes that the wireless radio channel consists of a set of discrete propagation paths (specular components or SCs). Additionally, the model also accounts for measurement imperfections by including a noise term that is assumed to be white in both the angular and delay domains. Recent work suggests to also include dense multipath components (DMC) to the signal model of estimation algorithms [3]. DMC originates from distributed scattering in the environment and is thought of as a part of the multipath profile that is continuous in both the angular and delay domains. DMC is modeled as an additive colored noise term and has been included in recently developed estimation algorithms, most notably RiMAX [3].

The physical reality of DMC raises the question how well estimation algorithms which historically do not include DMC into their signal model (ESPRIT, SAGE) estimate the SC part of the channel, and this compared to the performance of a DMC-inclusive estimation algorithm (RiMAX). This question is investigated in this letter.

Construction of channels including DMC: The physical environment chosen for synthesizing channels is a 66 m x 32 m x 10.8 m sports hall. In this environment, 1000 channels are constructed, where each channel corresponds to randomly chosen positions for the transmitting and receiving antennas. The sampled array response vector $h \in \mathbb{C}^{M_r M_t M_f \times 1}$ (where M_r, M_t, and M_f correspond to the numbers of receive antennas, transmit antennas, and frequency points, respectively) can be written as the sum of a deterministic SC part s and a stochastic DMC part d. It is assumed that h follows a multivariate circular symmetric complex Gaussian process [3]:

$$h = s(\theta_{SC}) + d(\theta_{DMC}) \text{ and } h \sim \mathcal{N}_C\big(s(\theta_{SC}), R(\theta_{DMC})\big) \quad (1)$$

To construct $s(\theta_{SC})$, ray-tracing is used to obtain the 50 strongest specular paths. The sports hall is modelled as a simple box-like structure for the ray-tracing simulations. Four parameters are associated with each SC (grouped into the parameter vector θ_{SC}), namely its Azimuth Of Arrival (AOA), Azimuth Of Departure (AOD), Time delay Of Arrival (TOA), and complex amplitude. On the other hand, $d(\theta_{DMC})$ is fully determined by the channel covariance matrix $R(\theta_{DMC})$. In recent models for the DMC, this covariance matrix is assumed to have the following structure involving Kronecker products [3]:

$$R(\theta_{DMC}) = I_{M_r} \otimes I_{M_t} \otimes R_f(\alpha_1, B_d, \tau_d, \alpha_0) \quad (2)$$

, where I represents the identity matrix. In (2), the dense field is modeled as white noise in the angular domains (I_{M_r} and I_{M_t}) and as colored noise in the time delay

domain ($\boldsymbol{R}_f$). The DMC power delay profile $\psi(\tau)$ as a function of time delay τ is typically described by an exponential decay:

$$\psi(\tau) = \alpha_1 e^{-B_d(\tau - \tau_d)} + \alpha_0 \qquad (3)$$

, where α_1, B_d, τ_d, and α_0 are four parameters which fully describe the DMC and are gathered into the DMC parameter vector $\boldsymbol{\theta}_{DMC}$. The DMC parameters were retrieved from channel sounding measurements in the sports hall reported in [4].

Following the construction of $\boldsymbol{\theta}_{SC}$ and $\boldsymbol{\theta}_{DMC}$, the array response vectors $\boldsymbol{h}$ are calculated according to (1). For this, 4x4 uniform rectangular antenna arrays were chosen at both receive and transmit side ($M_r = M_t = 16$). In addition, a 40 MHz bandwidth centered at 3.5 GHz was considered with a 1 MHz frequency step ($M_f = 41$). Finally, 10 independent observations of $\boldsymbol{h}$ were drawn for each channel. The channel construction process is repeated for three different ratios of the total DMC power P_{DMC} to the total SC power P_{SC}, namely P_{DMC}/P_{SC} equal to 0.3/0.7, 0.5/0.5, and 0.7/0.3. These ratios correspond to common distributions of power between the DMC and SC parts reported in literature [5].

Estimation of channel parameters: The SC parameter vector estimates $\widehat{\boldsymbol{\theta}}_{SC}$ were calculated with unitary ESPRIT, SAGE, and RiMAX for the 1000 constructed channels. It is noteworthy that the number of SCs the algorithm outputs has to be prespecified for ESPRIT and SAGE. On the other hand, RiMAX continues to search for new SCs until a convergence criterion is reached [3]. The ray-traced SCs with higher order reflections often display weak or negative signal-to-noise ratios. Hence, this results in some of the 50 ray-traced SCs not being detected and instead being classified as DMC. RiMAX resolved around 10000 out of 1000 times 50 ray-traced SCs. For the sake of fairness, the number of SCs detected by RiMAX was selected as input for ESPRIT and SAGE.

The pairing of each estimated SC with its exact ray-traced counterpart is done in terms of smallest Multipath Component Distance (MCD) between both [6]. To this end, each SC with parameter vector $\boldsymbol{\varphi}_{SC}$ is assigned a point x in a five-dimensional space:

$$x(\boldsymbol{\varphi}_{SC}) = \frac{1}{\sqrt{3}} \left[\frac{1}{2}\cos(AOA), \frac{1}{2}\sin(AOA), \frac{1}{2}\cos(AOD), \frac{1}{2}\sin(AOD), TOA/TOA_{max} \right]^T \quad (4)$$

The MCD between estimated $\widehat{\boldsymbol{\theta}}_{SC}$ and exact $\boldsymbol{\theta}_{SC}$ is calculated as the Euclidean distance between the corresponding points x, i.e., $MCD = \left\| x(\widehat{\boldsymbol{\theta}}_{SC}) - x(\boldsymbol{\theta}_{SC}) \right\|$. In (4), TOA_{max} is the maximum time delay of all estimated and exact SCs for each of the constructed channels.

Results: Figs. 1, 2, and 3 show the Complementary Cumulative Distribution Functions (CCDFs) of the absolute errors between AOAs, TOAs, and powers of estimated and ray-traced SCs. CCDFs are shown for each of the three estimation algorithms and each of the three P_{DMC}/P_{SC} ratios. As expected, the DMC-inclusive RiMAX algorithm exhibits better error performance (CCDFs shifted to the left) than the ESPRIT and SAGE algorithms. We note that SAGE returns slightly better angular estimates than ESPRIT (Fig. 1). Also, both estimators perform nearly identically for the TOA parameter (Fig. 2). Additionally, ESPRIT generally shows larger power estimation errors than SAGE (Fig. 3). This is because ESPRIT is only able to estimate the noise variance but not the noise's complex amplitude for each separate observation. This leads to approximations in the complex amplitude estimates of the SCs and hence to larger errors of estimated SC power. Furthermore, for all three algorithms the P_{DMC}/P_{SC} scenarios do not appear to have a large impact on the SC estimator performance. As expected, the effect of the P_{DMC}/P_{SC} ratio on RiMAX performance is almost nonexistent as this algorithm correctly accounts for DMC. For ESPRIT and SAGE, larger relative DMC power does not necessarily mean worse SC

estimates, showing that even at the largest P_{DMC}/P_{SC} ratio, the DMC power is not high enough to overshadow the strongest SCs in this simulation setup.

Table 1 shows SC parameter values corresponding to worst-case exceedance probabilities (i.e., the probability that an error occurs that is larger than that value) of 50, 10, and 1%. Three values are shown per parameter and exceedance probability, corresponding to estimations with the ESPRIT, SAGE, and RiMAX algorithms respectively. The values in Table 1 are averaged values taken over all three P_{DMC}/P_{SC} scenarios. From Table 1, it is clear that even at the larger, more forgiving exceedance probabilities of 50% and 10%, ESPRIT and SAGE show large errors compared to the relatively small errors exhibited by RiMAX.

Conclusion: The results of this study demonstrate that specular multipath component estimation in the presence of dense multipath components is prone to large estimation errors if the signal model is not accordingly modified in estimation algorithms such as ESPRIT and SAGE. Therefore, determining the DMC by subtracting the specular part, estimated by ESPRIT or SAGE, from the total channel response, as it is frequently done in literature, is flawed and must be avoided. For a faithful estimation of the SC and/or DMC parameters, the use of dense-multipath-inclusive algorithms like RiMAX is recommended.

References:

[1] M. Haardt. *Efficient One-, Two-, and Multidimensional High-Resolution Array Signal Processing*. PhD thesis, Technische Universität München, Shaker Verlag GmbH, Aachen, DE, 1996.

[2] B. H. Fleury, M. Tschudin, R. Heddergott, D. Dahlhaus, and K. I. Pedersen. *Channel Parameter Estimation in Mobile Radio Environments Using the SAGE Algorithm*. IEEE Journal on Selected Areas in Communications, 17(3):434–450, March 1999.

[3] A. Richter. *Estimation of Radio Channel Parameters: Models and Algorithms*. PhD thesis, Technische Universität Ilmenau, Fakultät für Elektrotechnik und Informationstechnik, Ilmenau, DE, 2005.

[4] E. Tanghe, W. Joseph, M. Liénard, A. Nasr, P. Stefanut, D. P. Gaillot, P. Degauque, and L. Martens. *Clustering of Channel Parameters by Block Diagonal Matrix Decomposition.* In COST 2100 7th Management Committee Meeting, Braunschweig, DE, February 2009.

[5] J. Salmi, J. Poutanen, K. Haneda, A. Richter, V.-M. Kolmonen, P. Vainikainen, and A. F. Molisch. *Incorporating Diffuse Scattering in Geometry-based Stochastic MIMO Channel Models*. In 4th European Conference on Antennas and Propagation, Barcelona, ES, April 2010.

[6] M. Steinbauer, H. Özcelik, H. Hofstetter, C. F. Mecklenbräuker, and E. Bonek. *How to quantify multipath separation*. IEICE Transactions on Electronics, E85-C(3):552–557, 2002.

Authors' affiliations:

E. Tanghe, W. Joseph, and L. Martens (Ghent University / IBBT, Dept. of Information Technology, Gaston Crommenlaan 8 box 201, B-9050 Ghent, Belgium)

D. P. Gaillot, M. Liénard, and P. Degauque (University of Lille, IEMN, Group TELICE, Bldg. P3, F 59655 Villeneuve d'Ascq, France)

E-mail: emmeric.tanghe@intec.ugent.be

Figure captions:

Fig. 1   CCDFs of absolute AoA estimation error

Fig. 2   CCDFs of absolute ToA estimation error

Fig. 3   CCDFs of absolute power estimation error

Table captions:

Table 1   average errors corresponding to exceedances of 50, 10, and 1% (cell key: ESPRIT|SAGE|RiMAX)
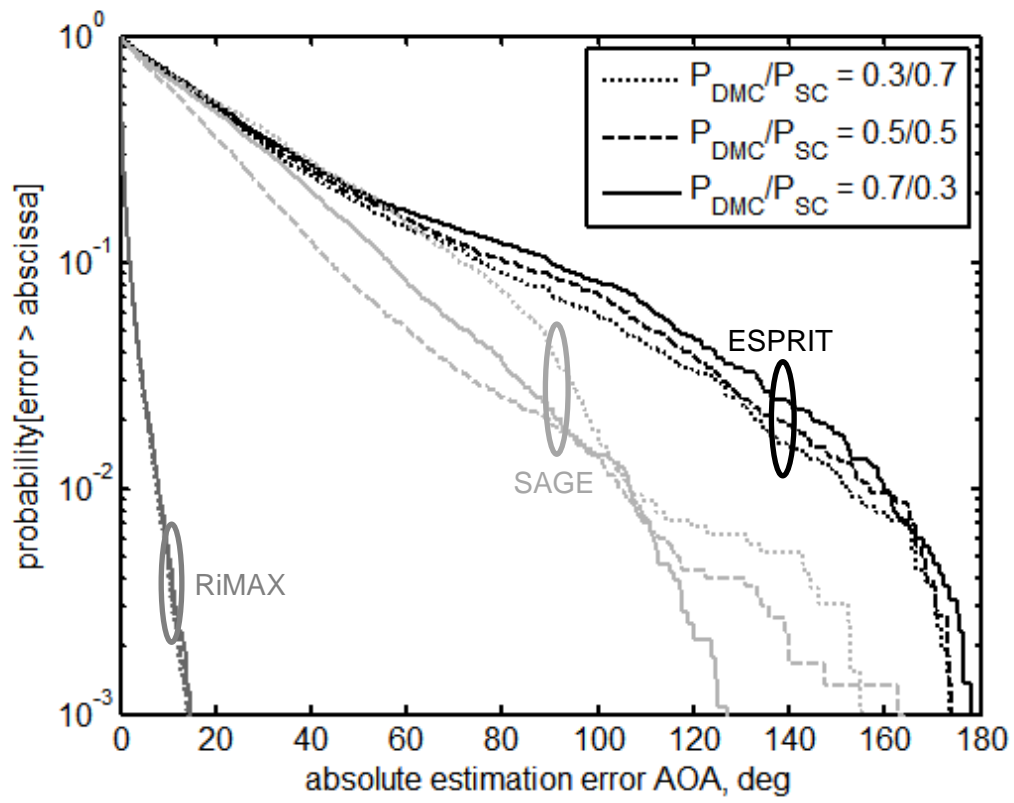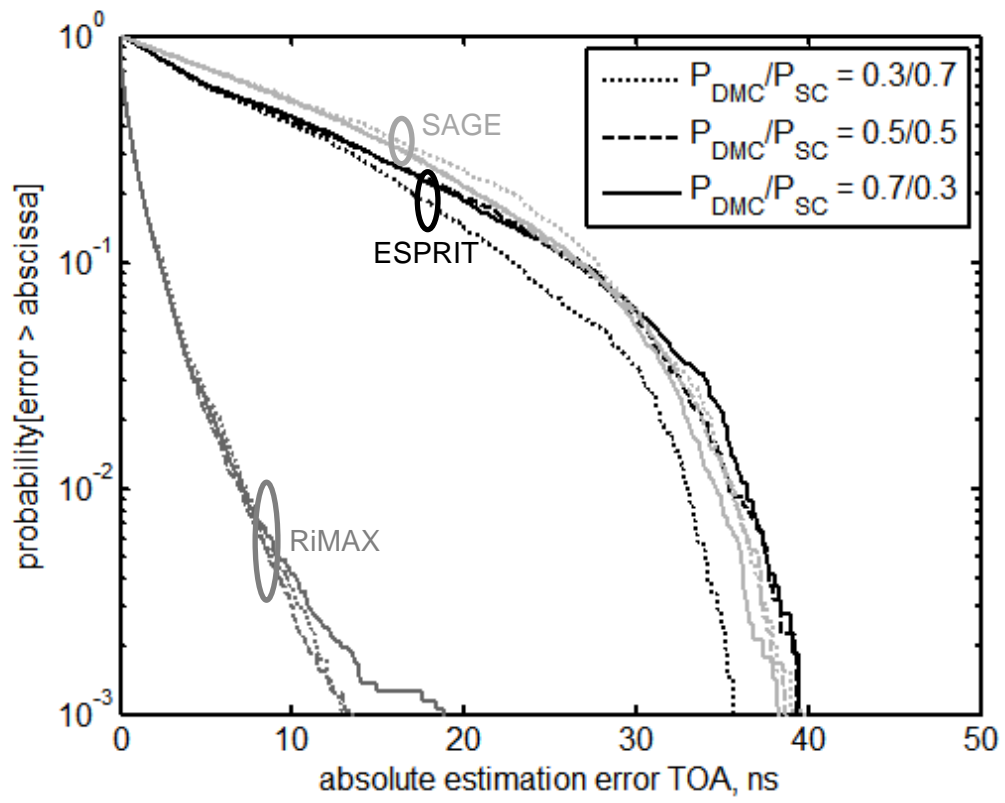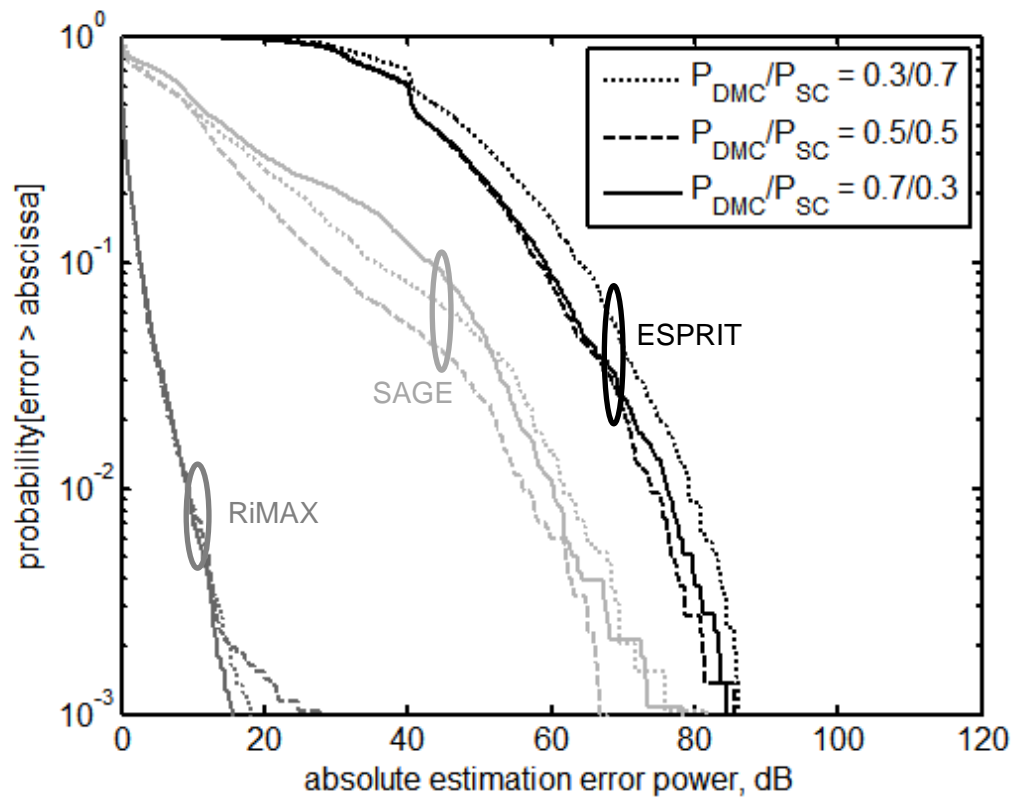
Figure 1

Figure 2

Figure 3

Table 1

Exceedance	50%	10%	1%
AOA, deg	19.7|17.4|0.3	82.2|57.2|2.1	156.0|106.0|7.9
AOD, deg	21.9|15.6|0.2	108.9|71.8|1.6	171.3|128.3|6.3
TOA, ns	7.7|10.5|0.3	25.3|27.0|2.4	35.0|35.3|7.1
power, dB	41.6|9.8|0.2	60.4|35.8|2.7	76.4|59.4|9.3